

Current-meter flow rate measurement using the moving frame method

N. Gloor¹, T. Staubli¹, A. Abgottspon¹, Y. Cho²

¹*etaeval GmbH, 6048 Horw, Switzerland*

²*K-Water, 34045 Daejeon, South Korea*

nicolas.gloor@etaeval.ch

Abstract

Velocity distributions in the intake of low-head hydroelectric power plants (HPPs) can be measured either with a large number of propeller-type current-meters mounted on a frame throughout the flow cross-section, or with current-meters mounted on a subframe that is moved stepwise to various vertical or horizontal positions, or by moving the subframe continuously through the measuring section. The moving frame method being about 10 times faster than the stepwise method and thus brings an important time advantage.

The experience gathered with the stepwise moved and the continuously moving frame during a field test in HPP Hapcheon 2, South Korea are presented. Six comparative measurements were performed and show the excellent suitability of the moving frame method. The average difference of the two integrated flow rates is in the order of 0.1%. To achieve this result, the angle of incidence of the flow with respect to the axis of the current-meter during the movement of the frame must be considered.

1. Introduction

There are a multitude of flow rate measuring methods in closed conduits. For low-head hydroelectric power plants (HPPs) with short intakes, however, propeller type current-meters are often the best solution to measure the velocity distribution and from this to compute the flow rate. The method has good measurement accuracy, typically in the range of ± 1.0 to 2.0% , when the current-meters are previously calibrated in a towing tank. Self-compensated propellers of current-meters allow deviation of the flow direction up to 5° from the propeller axis without correction of the measured velocity [1]. The methods for measuring the velocity distributions and integrating the flow rate are described in the standards IEC 60041 “Field acceptance tests to determine the hydraulic performance of hydraulic turbines, storage pumps and pump-turbines” [1] and in ISO 3354 “Measurement of clean water flow in closed conduits” [2].

To measure the velocity distribution in a flow cross-section, either a large number of current-meters can be installed on a frame covering the entire flow cross-section, or a reduced number of current-meters mounted on a subframe are successively positioned in a stepwise manner to different vertical or horizontal positions. In both methods, current-meters record the local point velocities for a specified period of time, which can last up to several minutes depending on flow conditions. The advantage of the first method is the shortest possible acquisition time per measuring point, disadvantages are the large installation effort and the high costs. In the second method, the velocity distribution is recorded step by step by moving the frame in the measuring cross-section from one position to another. This is correspondingly much more time-consuming. The net measurement duration for the entire cross-section is considerable and can be up to one and a half hour, depending on the conditions on site. [3]. To save time, an alternative method is to move the current-meters with constant speed through the measuring cross-section while continuously recording the flow velocity. In the following, this method will be referred to as the “moving frame method”. Hereby, the flow field is measured by moving the current-meters at constant speed along a vertical or horizontal line of the measuring cross-section.

In the field experiment presented here, the velocity distribution was measured by moving the current-meters vertically through the flow cross-section at a constant velocity. In this way, a vertical velocity distribution over height is measured for each current-meter. Even if the frame speed is low, a constant incidence deviation must be compensated for.

This method is also mentioned in earlier publications as “moving frame” [4, 5] or “profiling” [6, 7] method. There is little normative information on such measurements in ISO 3354 under 7.3.2. “Exploration of a section by means of a row or current-meters”. The following content focuses on the integration method of the data with the stepwise positioned frame and of the data acquired with the moving frame and comparison of both results. The analysed data have been collected during the field tests in HPP Hapcheon 2, South Korea in October 2019.

2. Installation setup

2.1 Layout and flow condition

Low-head HPPs are often characterised by a short intake section. The Figure 1 (left) shows the situation at HPP Hapcheon 2. The streamlines on the surface are easily recognisable due to the turbidity of the water. In the reservoir upstream of the first trash rack the streamlines follow the river. In between the two trash racks the streamlines are bent towards the intakes and turbulent structures are observable in the flow. Local flow separation at the piers can be spotted.

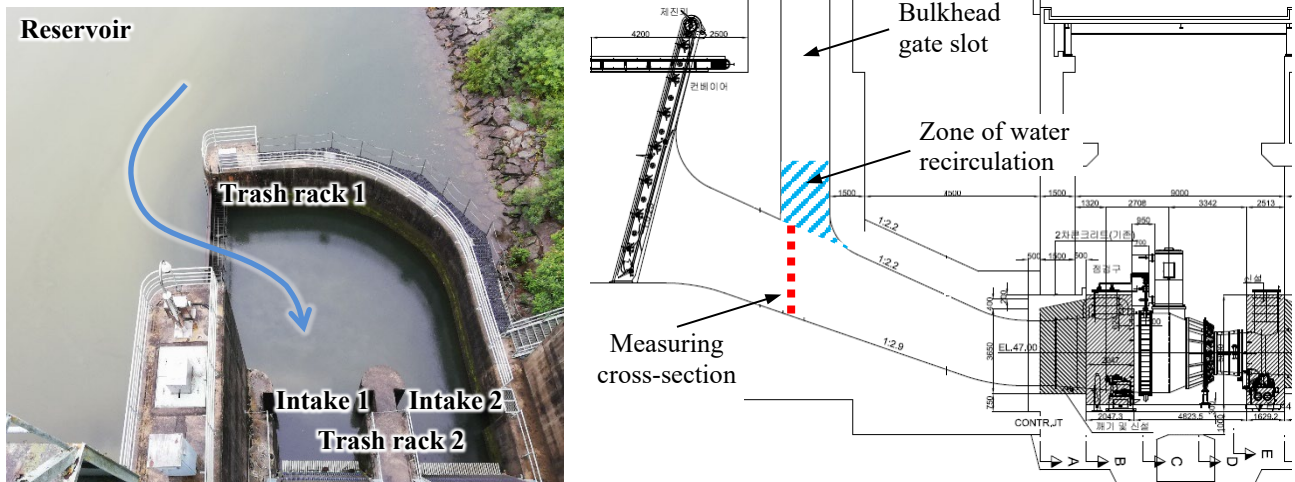


Figure 1: Top view of the intake zone of HPP Hapcheon 2, South Korea (left). Turbine intake with the measuring cross-section and recirculation zone in the bulkhead gate slot (right).

The Figure 1 (right) shows a side view of the intake. The convergence of the intake generates an accelerated flow at the position of the measuring cross-section. Accelerated flows delays the formation of a fully developed velocity profile. This leads to extended boundary layers and must be taken into account when calculating the near-wall velocity with a suitable wall exponent. For accelerated flows, this exponent typically becomes large. Due to the plant layout, the streamlines are crossing the measuring section at an average angle of 21.74° . Current-meters on the measuring frame were aligned to this slope. The upper part of the measuring cross-section is open to the bulkhead, and water recirculation in this zone potentially affects the velocity distribution at the top of the integration area.

2.2 Current-meter frame

At the HPP Hapcheon 2, the most practical way to perform the measurements of the flow velocity was in the bulkhead gate opening. A transversal frame with rollers fitting into this opening was built to carry the current-meters. The current-meters are distributed over the width of the frame respecting the ISO 3354. To perform the measurement, the frame is hooked onto the crane and inserted through the bulkhead opening into the intake. Once the frame is placed at the start position, the acquisition of the velocities is started, and the frame is moved by crane through the section until the upper or lower end, depending on the start position, is reached.

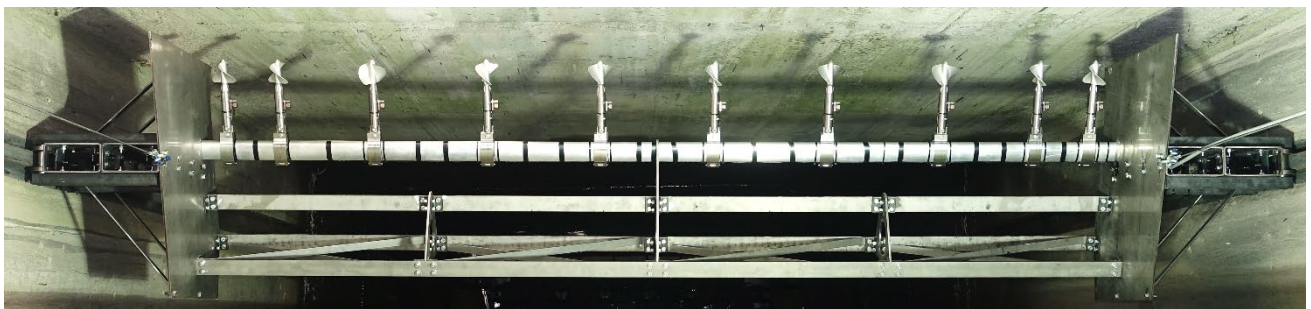


Figure 2: Installation of the measuring frame. View through the bulkhead gate slot at HPP Hapcheon 2.

3. Stepwise and moving frame measuring methods

According to the standard IEC 60041 [1] the number of measuring points, Z , shall be determined from:

$$24 \cdot \sqrt[3]{A} < Z < 36 \cdot \sqrt[3]{A} \quad (1)$$

The measuring cross-section is 4 m (height) times 3.4 m (width) = 13.6 m². Therefore, the number of local velocity measurements should be $57 < Z < 86$. It was decided to mount 10 current-meters on the horizontal profile. With stepwise measurements on 9 elevations this results in 90 measuring points. The ninth elevation is set close to the upper boundary of the measuring section, to get more information on the velocity gradient near the water separation line of the recirculation zone.

Moving frame data were acquired for a series of operating points directly after the stepwise data measurements during the efficiency measurement campaign. Therefore, the operating conditions of the turbine remained unchanged for both types of measurement.

In the HPP Hapcheon 2, the crane speed was measured to be 0.01754 m/s. This results in a measuring time of about 3.4 minutes for a moving frame measurement. In contrast, the stepwise measurements took at least 3 minutes per measuring layer. Considering the 9 layers plus the time for the frame displacement, the measuring duration resulted in about 30 minutes. The moving-frame method thus offers a major advantage in terms of time savings compared with the stepwise method.

The moving frame measurements were conducted from top to bottom or from bottom to top depending on the final position of the frame after the previous measuring point. In total 3 points were measured from top to bottom and 3 others from bottom to top with the moving frame method. The instantaneous vertical position of the current-meters could not be acquired during the measurements, which means that the start and end of the measurements had to be defined manually with marks on the crane rope for the evaluation of the results. The vertical position of the current-meters was then calculated with the speed of the bulkhead gate, which was very constant. The crane speed of 0.01754 m/s corresponded to 4.4% of the mean flow velocity at the lowest operating point. This percentage decrease with increasing flow velocity. According to ISO 3354, sections 7.2.2 Rotating arm and 7.3.2 Exploration of a section by means of a row of current-meters, the motion speed shall not exceed 5% of the mean flow velocity.

The rotational frequency of each current-meter was evaluated after each revolution (1 impulse per revolution). The read-out rate of this frequency was with 20 values per second much higher. Thus, the same frequency appeared in the data transmitted to the acquisition system until a new complete revolution of the current-meter occurred. Using the instantaneous frequency and the calibration equation of the current-meter, the instantaneous flow velocity could be determined. The current-meters used have a slope of 0.25 m/rev. Assuming a velocity of 1.25 m/s, this results in five revolutions per second. During data acquisition with 20 values per second, therefore the same frequency is recorded four times until a new value is refreshed.

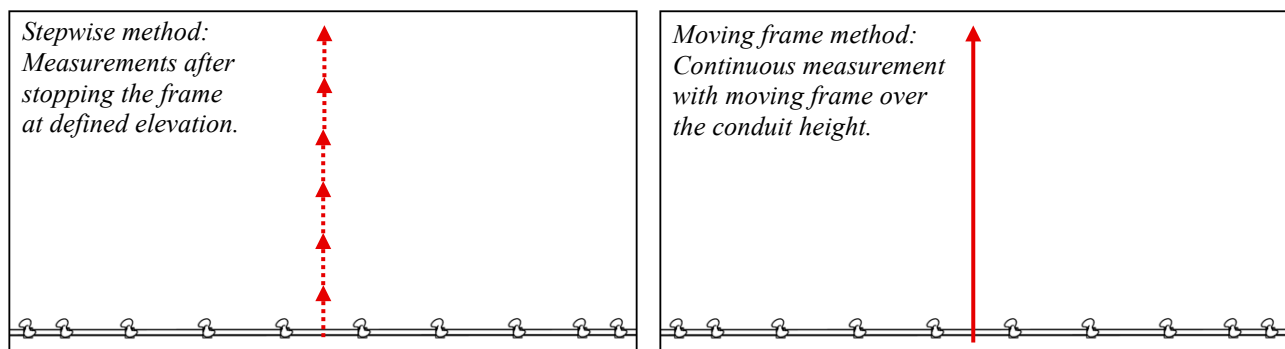


Figure 3: Example of a vertical arrangement at the measuring cross-section for the stepwise method according to ISO 3354 (left) and with moving frame method (right).

4. Flow rate calculation

4.1 Flow rate

The flow rate of the measured cross-section is given by Equation (2).

$$Q = v_{mean,normal} \cdot A \quad (2)$$

Q flow rate [m³/s]
 $v_{mean,normal}$ mean velocity normal to the cross-section [m/s]
 A area of the cross-section [m²]

4.2 Integration of the velocity differences

The method described in [8] is called integration method of the differences with respect to a reference flow rate. Such a reference flow rate can be determined from CFD simulations or from integration of analytical velocity distributions. This

method particularly suits to generally shaped flow cross-section that are not described in the standards. It possesses a higher integration accuracy because it does not have to handle the exponential behaviour of the boundary layer flow. In the analytical approaches, the power law and its exponent should be chosen so that the measurements are well approximated.

Figure 4 shows for example measured velocity over the conduit length (x) at the middle elevation (y) of the conduit. In this case, the horizontal power law velocity is calculated for the same elevation. The horizontal power law profile changes his shape in function of his vertical position and is computed with Equation (2). The measured velocity is subtracted to the power law to build the velocity difference and finally the velocity difference is integrated, based on cubic interpolation between data points, as described in ISO 3354.

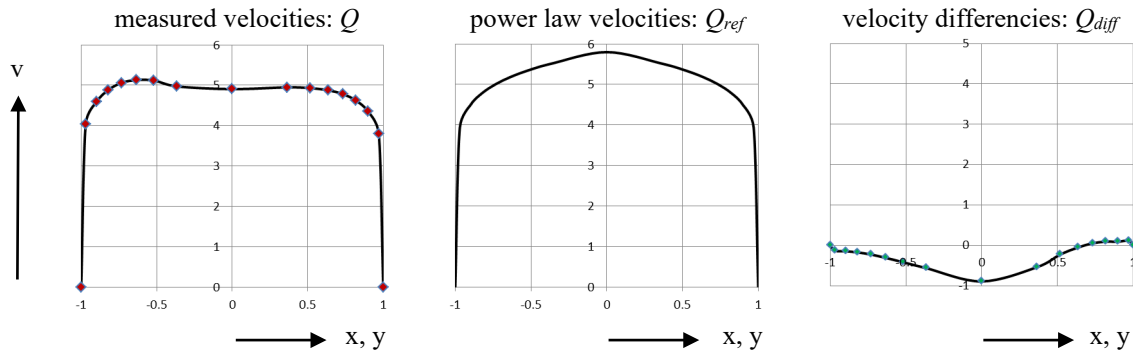


Figure 4: Integration method of velocity differences: $Q = Q_{ref} - Q_{diff}$ [8].

The power law velocity profile for rectangular cross-section is calculated with Equation (3) [8].

$$v(x, y) = v_{max} \left(1 - \frac{|x|}{W/2}\right)^{\frac{1}{n}} \left(1 - \frac{|y|}{H/2}\right)^{\frac{1}{m}} \quad (3)$$

- v_{max} maximum velocity [m/s]
- W conduit width [m]
- H conduit height [m]
- n wall exponent of the side wall [-]
- m wall exponent of the top and bottom [-]

For the analytical computation of the flow rate the power law is integrated with Equation (4) [8].

$$Q_{ref} = v_{max} \cdot W \cdot H \cdot \frac{n \cdot m}{(1 + n) \cdot (1 + m)} \quad (4)$$

Q_{ref} Reference flow rate of the power law [m^3/s]

4.3 Wall exponent

According to ISO 3354 a well-developed flow profile is characterized by a wall exponent of 4 to 14. In the case of the measurements at the HPP Hapcheon 2, the situation on site does not meet the requirements for fully developed flow conditions. The actual wall exponent is approximated by Equation (5) according to the procedure described in ISO 3353 in Annex E [2]. Equation (5) shows the approximation for the x-direction. For the y-direction, x is replaced in Equation (5) by y , W by H , and n by m .

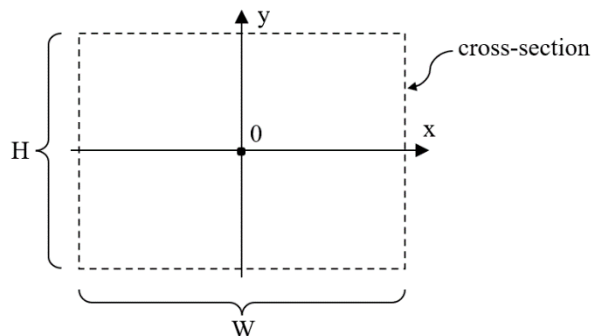


Figure 5: Reference system for the computation of the wall exponent of a rectangular cross-section.

$$\frac{1}{n} = \operatorname{atan} \left(\frac{\log \left(\frac{v_1}{v_{ref}} \right) - \log \left(\frac{v_2}{v_{ref}} \right)}{\log \left(1 - \frac{|x_1|}{W/2} \right) - \log \left(1 - \frac{|x_2|}{W/2} \right)} \right) \quad (5)$$

- v_1 measured velocity closest position to the wall [m/s]
- v_2 measured velocity at the second closest position to the wall [m/s]
- v_{ref} reference velocity [m/s], normally the maximal velocity or in a dimensionless representation 1
- x_1 x-position of measured velocity 1 [m]
- x_2 x-position of measured velocity 2 [m]

The Figure 6 shows the wall exponent evaluated along the periphery of the measuring section. The colour represents the value of the wall exponent. On the right and left sides and on the upper part of the section, the exponent varies from 20 to 35. An average wall exponent of 30 was selected for the integration of the flow rate Q_{ref} . Such a high value confirms that the exponential increase of velocity near the wall is steeper than for a fully developed velocity profile. On the bottom, the wall exponent was evaluated as negative. This means that the measured velocities increase towards the bottom down to the last row of measured velocities. Due to plant restrictions, the current-meters could not be positioned close enough to the conduit bottom to reach the expected exponential velocity decrease. For this reason, also at the bottom a wall exponent of 30 was selected.

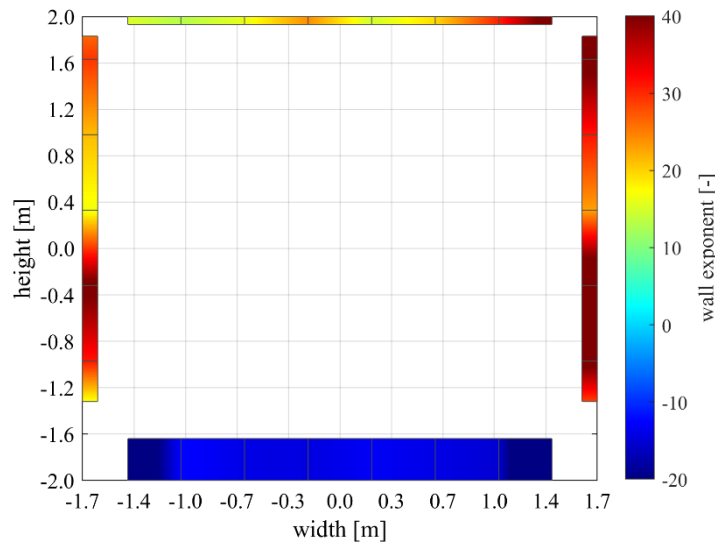


Figure 6: Evaluated wall exponent along the periphery of a representative operating point.

4.4 Incidence angle correction

Any relative motion of the current-meter in a flow leads to a modification of the incidence angle φ with respect to the axis of the current-meter. The response of self-compensated current-meter readings on an incidence angle follows to a good approximation a cosine law, Equation (6). Figure 7 shows the cosine law and measurements with the R-impeller current-meter from Ott company [10]. At an angle of incidence of 5° , for example, the current-meter indicates a velocity that is 0.38% too low without correction.

$$\frac{v}{v_0} = \cos(\varphi) \quad (6)$$

- v velocity at incidence φ [m/s]
- v_0 velocity at incidence $\varphi = 0$ [m/s]
- φ incidence angle [$^\circ$]

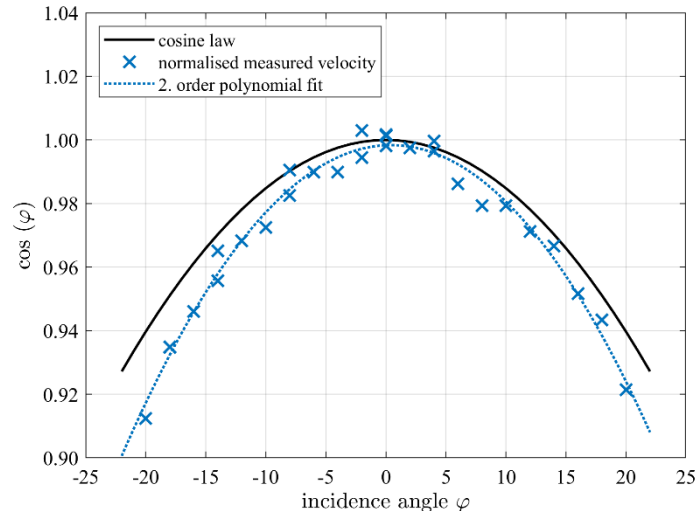


Figure 7: Cosine law and normalised measured velocity as a function of the incidence angle for measurements with the R-impeller current-meter from Ott company [10].

Equation (7) show the correction of the measured velocity as a function of the incidence angle. In the case of the measurements in HPP Hapcheon 2, the incidence angle φ under motion of the current-meter varied between 0.93° at the highest measured flow rate (95% of $P_{nominal}$) and 2.28° at the lowest measured flow rate (40% of $P_{nominal}$). Due to cosine law, this results in a correction of the current-meter reading from 0.013% at full load to 0.079% at part load and was considered consequently.

$$v_{relative} = \frac{v_{measured}}{\cos(\varphi)} \quad (7)$$

$v_{measured}$ measured velocity at incidence φ [m/s]
 $v_{relative}$ relative velocity at incidence $\varphi = 0$ [m/s]

4.5 Calculation of the normal velocity component

According to section 4.1 the normal component v_{normal} to the measuring cross-section of the relative velocity $v_{relative}$ is needed to compute the flow rate Q . Figure 8 shows the local flow velocity v_{flow} relative to the axis of the current-meter. For the steady state measuring setup (fixed frame, Figure 8 left) the incidence angle φ is assumed to be in the average zero, since with the inclination angle α of 21.74° of the current-meters, no correction of the incidence angle φ is needed and the relative velocity $v_{relative}$ corresponds to the flow velocity v_{flow} . In this case the normal velocity component v_{normal} is calculated with the inclination angle α . When the frame moves, the direction of the relative velocity $v_{relative}$ changes proportionally to the frame velocity v_{frame} and as well as the angle of incidence φ between the flow velocity and the axis of the current-meter. Thus, the incidence angle increases during downward movement (Figure 8 middle) and decreases during upward movement (Figure 8 right). The angle φ under motion condition is calculated using the Equations (8 and 9). Without correction of the incidence angle, a downward shift of the frame would result in a higher reading of the velocity. In the opposite direction, an upward movement would result in a lower reading of the velocity. These influences on the incidence and on the associated normal velocity component had to be considered for the flow rate determination with a moving frame.

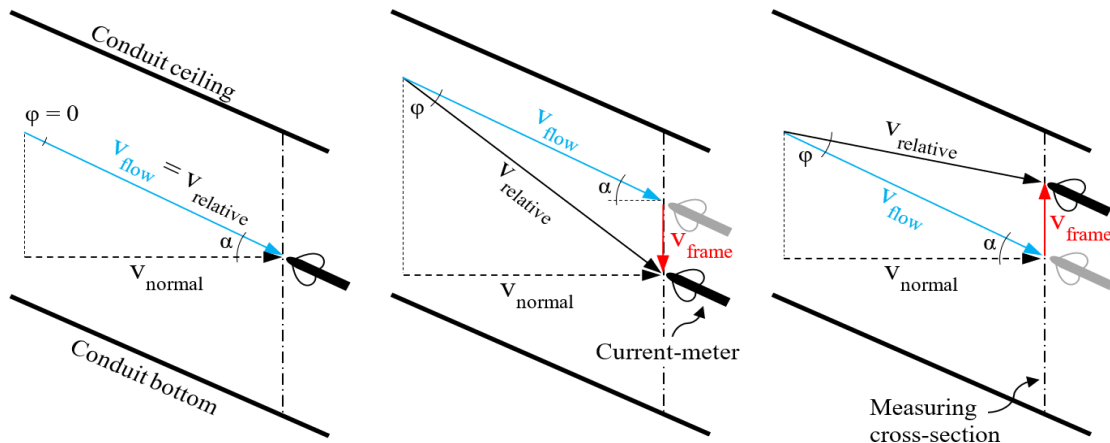


Figure 8: Velocity vectors and angles definitions: Fixed position of the frame (left), downward motion of the frame (middle), upward motion of the frame (right).

The incidence angle under motion φ for downward and upward displacement is calculated as follows:

$$\sin(\varphi_{down}) = \frac{v_{frame}}{v_{relative}} \cdot \sin(\alpha + 90) \quad (8)$$

$$\sin(\varphi_{up}) = \frac{v_{frame}}{v_{relative}} \cdot \sin(90 - \alpha) \quad (9)$$

The normal velocity component v_{normal} is calculated as:

$$v_{normal,down} = v_{relative,down} \cdot \cos(\alpha + \varphi) \quad (10)$$

$$v_{normal,up} = v_{relative,up} \cdot \cos(\alpha - \varphi) \quad (11)$$

4.6 Velocity distribution

The interpolated velocity distribution at the largest measured flow rate is shown in the Figure 9. A bi-cubic interpolation algorithm is used in both stepwise (left) and the moving frame (right) methods. The velocity gradient in vertical direction of the stepwise method is smoother than the gradient of the moving frame method due to the smaller amount of measuring points. The boundary layers with velocities decreasing to zero (blue colour) are apparent along the periphery of the rectangular cross-section. The maximal velocities are observed towards the bottom part of the section.

The black dots on the left graph show the position of the individual current-meters during the measurement with the stepwise method. The vertical lines on the right graph represent the paths of the current-meters during the moving frame measurement. The velocity profile along one of the marked lines is depicted in Figure 10.

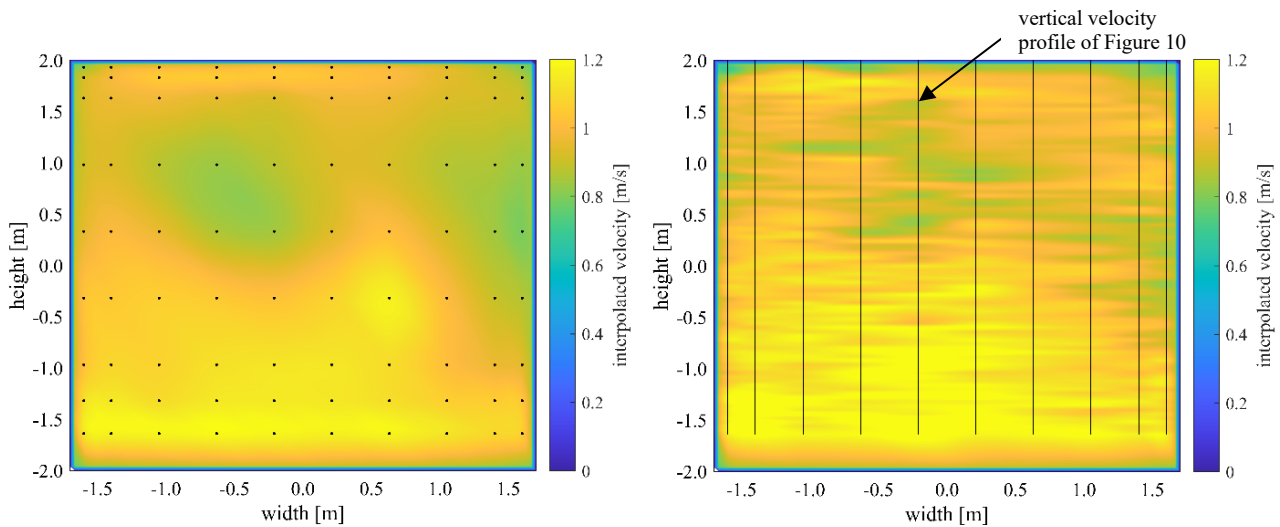


Figure 9: Interpolated velocity profile in the cross-section of a representative operating point. Left: Stepwise method. Right: Moving frame method. Dots and Lines: Locations of the measured velocities.

Because of the bulkhead gate opening on the top, the boundary condition differs from that of the fixed walls with zero velocity. In the bulkhead gate slot, a recirculation zone of water caused above the measuring section. This type of flow is e.g. described and simulated with CFD in [4]. At the leading edge of the opening, the flow is characterised by a shear layer with a steep velocity gradient. With increasing distance from the leading edge, the velocity gradient becomes smaller. To avoid additional uncertainties the current-meters were positioned as close as possible to the leading edge. The moving frame measurements through this shear layer zone in Figure 10 show the steepness of the gradient, although the current-meter averages the velocities due to its size.

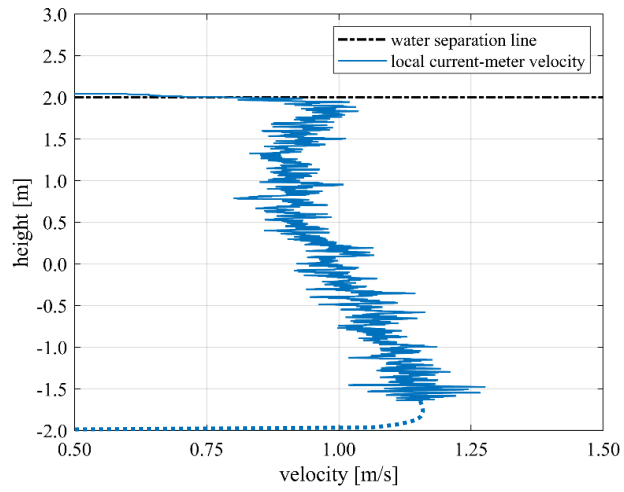
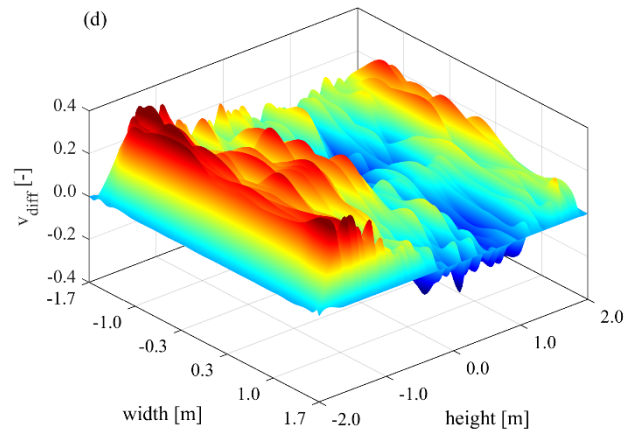
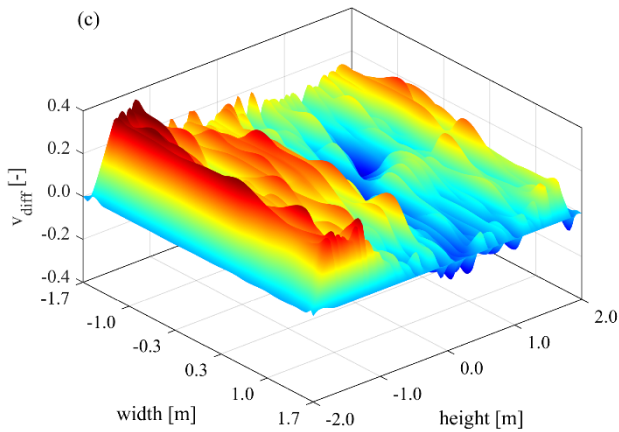
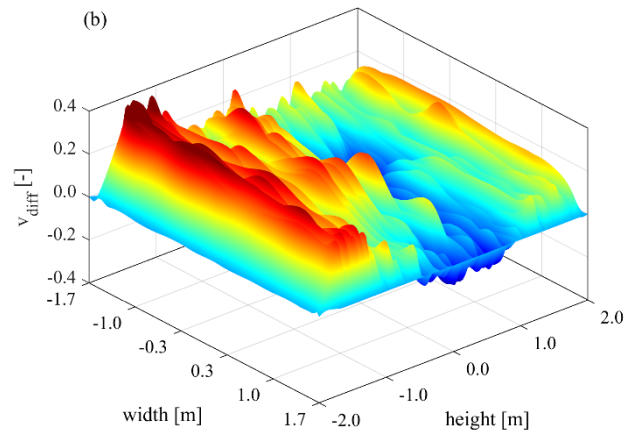
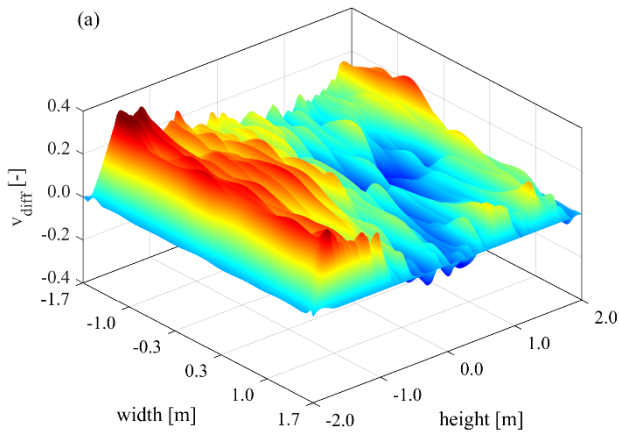


Figure 10: Vertical velocity profile crossing the water separation line of the recirculation zone above the measuring cross-section of a representative operating point. Blue dots: extrapolated velocity.

The normalised velocity difference v_{diff} is defined as in Equation (12).

$$v_{diff} = \frac{v_{normal}}{v_{mean,normal}} - v_{power\ law} \quad (12)$$

v_{diff} normalised velocity difference [-]
 $v_{mean,normal}$ mean velocity normal to the cross-section [m/s]
 $v_{power\ law}$ normalised power law velocity [-]



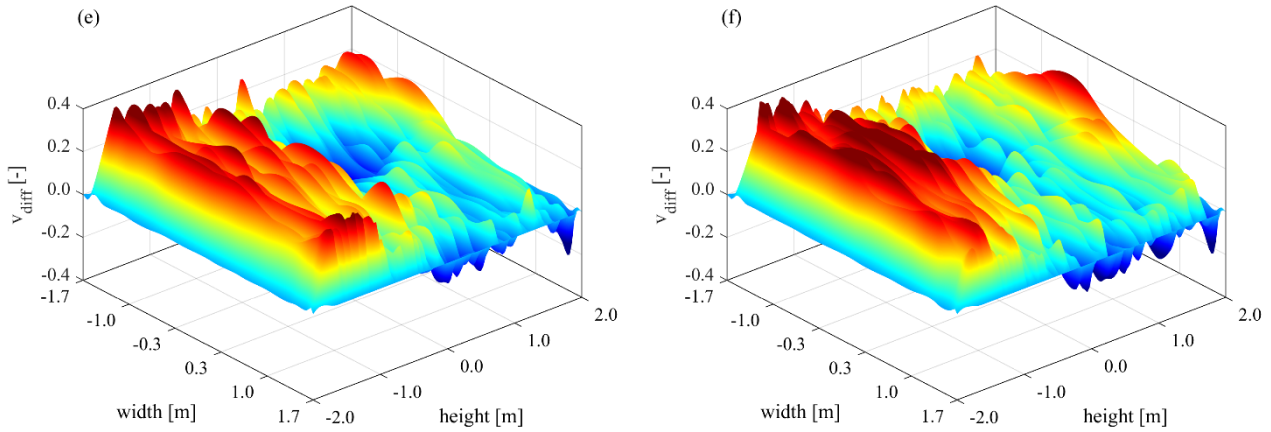


Figure 11: Profile of the normalised velocity difference at various operating points.
 a = 95% of P_{nominal} , b = 80%, c = 70%, d = 60%, e = 50%, f = 40%

5. Results

The velocity differences according to Equation (12) are shown in Figure 11 for six operating points with decreasing flow rates. The integration of the corresponding areas results in the flow rate Q_{diff} . From this integral the flow rate Q is determined, as described in section 4.2 and illustrated in Figure 4. The deviations of the flow rates of the two methods (stepwise and moving frame) after correction of the angle of incidence are between -0.07% and 0.07%. It is not clear if there is a systematic influence of the upward or downward motion of the frame. It should be noted that the stepwise measurements and moving frame measurements were carried out one after the other and minor variations of the flow conditions might have occurred in between the two measurements.

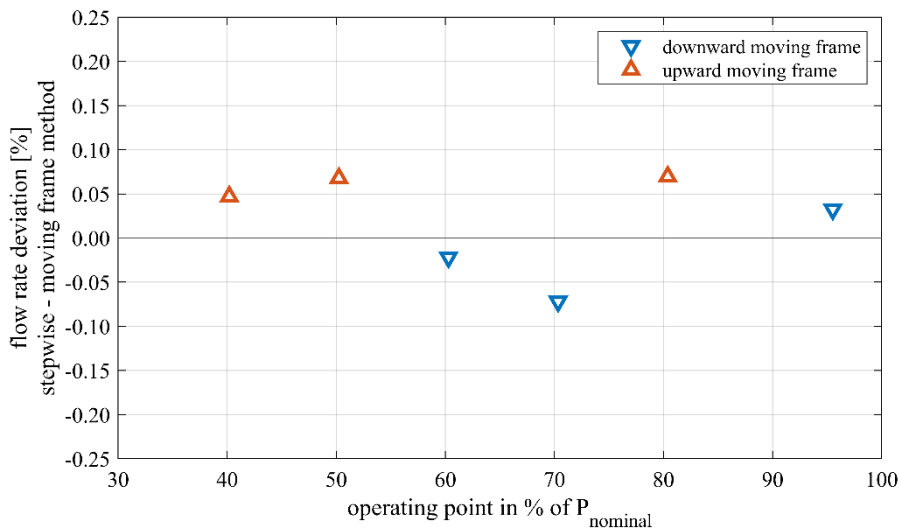


Figure 12: Flow rate deviation of the stepwise and the moving frame method.

6. Conclusion

Current-meter measurements were undertaken in a short and convergent turbine intake. Local velocity distributions of six turbine operating points were measured both with the stepwise method and with the moving frame method. The flow rates for both methods were evaluated using the integration method of velocity differences. Although the measurements were performed with both methods consecutively, i.e. with a certain time shift in between, the deviation of the stepwise method and the moving frame method varied only between -0.07% and 0.07% depending on the operating point. Whether there is a systematic influence of the direction of the frame movement could not be conclusively clarified.

The six chosen operating points covered a range of 40% to 95% of the nominal power. The distributions of normalised velocity differences have basically the same shape for all operating points. This leads to the conclusion that the flow field in the turbine intake has not changed significantly with power.

The measuring time for one flow rate with the moving frame method was about 3.4 minutes, 10 times faster than the stepwise measurements with about 30 minutes per flow rate. The moving-frame method thus offers a major advantage in terms of time savings compared with the stepwise method. A prerequisite for the moving frame method is that a crane with a slow lifting speed is available. In addition, the crane must ensure constant movement.

Acknowledgements

The authors thank K-Water and the staff of HPP Hapcheon 2 for their excellent support during the measuring campaign.

References

- [1] IEC 60041: "Field acceptance tests to determine the hydraulic performance of hydraulic turbines, storage pumps and pump-turbines." 3rd ed., IEC, Geneva, 1991.
- [2] ISO 3354: "Measurements of clean water in closed conduits. Velocity-area method using current-meters in full conduits and under regular flow conditions." 3rd ed., ISO, Geneva, 2008.
- [3] Staubli T., Abgottspon A.: "Discharge measurement in low head hydro power plants" Intl. Conf. on Energy and Environment (CIEM), Bucharest, Romania, 2017.
- [4] Proulx G.: "Kootenay canal plant comparative flow measurements: Current-meter method" Hydro-Québec, Montréal, Québec, Canada, 2010.
- [5] Proulx G., Cloutier E., Bouhadji L., Lemon D.D.: "Comparison of discharge measurement by current meter and acoustic scintillation methods at La Grande-1" in *Proc. 5th Intl. Conf. on Hydraulic Efficiency Measurements (IGHM)*, Lucerne, Switzerland, 2004.
- [6] Lemon D.D., Caron N., Cartier W.W., Proulx G.: "Comparison of turbine discharge measured by current meters and acoustic scintillation flow meter at Laforge-2 power plant" in *Proc. 2th Intl. Conf. on Hydraulic Efficiency Measurements (IGHM)*, Reno, United States of America, 1998.
- [7] Almquist C.W.: "Short converging intake comparative flow rate measurement tests at Kootenay Canal", CEATI Project No. T092700-0358, Centre for Engineering Advancement through Technological Innovation, Montréal, Québec, Canada, 2011.
- [8] Staubli T., Von Burg M., Abgottspon A.: "Integration of current-meter measurements in general flow cross section" in *Proc. 10th Intl. Conf. on Hydraulic Efficiency Measurements (IGHM)*, Itajubá, Brazil, 2014.
- [9] Wippermann R.: "Beitrag betreffend das Verhalten von Messflügeln bei Schräganströmung" in *Proc. 7th International Current-Meter Group (ICMG)*, Bologna, Italy, 1965.
- [10] Gloor N.: "Exploration of a new current-meter design", Bachelor thesis, Lucerne School of Engineering and Architecture, Lucerne, 2020.